

An Image Understanding System Using Attributed Symbolic Representation and Inexact Graph-Matching

M. A. ESHERA, MEMBER, IEEE, AND KING-SUN FU, FELLOW, IEEE

Abstract—This paper presents a powerful image understanding system that utilizes a semantic-syntactic (or attributed-symbolic) representation scheme in the form of attributed relational graphs (ARG's) for comprehending the global information contents of images. Nodes in the ARG represent the global image features, while the relations between those features are represented by attributed branches between their corresponding nodes. The extraction of ARG representation from images is achieved by a multilayer graph transducer scheme. This scheme is basically a rule-based system that uses a combination of model-driven and data-driven concepts in performing a hierarchical symbolic mapping of the image information content from the spatial-domain representation into a global representation. Further analysis and interpretation of the imagery data is performed on the extracted ARG representation. A distance measure between images is defined in terms of the distance between their respective ARG representations. The distance between two ARG's and the inexact matching of their respective components are calculated by an efficient dynamic programming technique. The system handles noise, distortion, and ambiguity in real-world images by two means, namely, through modeling and embedding them into the transducer's mapping rules, as well as through the appropriate cost of error-transformation for the inexact matching of the ARG image representation. Two illustrative experiments are presented to demonstrate some capabilities of the proposed system. Experiment I deals with locating objects in multiobject scenes, while Experiment II is concerned with target detection in SAR images.

Index Terms—Attributed graph, attributed symbolic representation, graph distance measure, graph matching, hierarchical knowledge representation, image understanding, scene analysis.

I. INTRODUCTION

THERE are two major stages in most machine vision and image understanding systems, as shown in Fig. 1 [5]. The first stage is concerned with the extraction of an adequate and efficient form of knowledge representation from the imagery data. In the second stage, the actual analysis and processing of the image is performed, usually on the extracted representation. Several forms of image representation have been used in image analysis, in general, and in the structural approach in particular.

For an image understanding system to be practical, it should be able to handle at its input the real-world images themselves, or at most, the output of some simple preprocessing operations. It must comprehend the image infor-

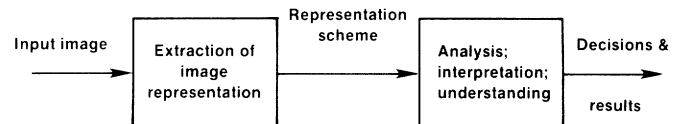


Fig. 1. Basic components of a general computer vision and image understanding system.

mation contents and preserve all its useful properties, such as symmetry, closure of curves, connectivity, etc., throughout the different stages of processing. It should also be able to handle noise, distortion, and uncertainty which almost always exist in real-world images.

Traditionally, there have been two major approaches to global image representation, namely, the parametric approach and the syntactic approach. In the parametric approach, objects are represented by vectors of features, e.g., color, size, etc., which can be easily measured from images. This is usually the basic form of image representation used in the decision-theoretic approach to pattern recognition [10]. On the other hand, in the syntactic representation, image features are represented as sets of symbolic entities, or an alphabet of image primitives. The structural relations between these features are represented by mutual relations between symbols of the alphabet [7], [14].

A more powerful approach for image representation has been emanating from the syntactic approach by combining the parametric approach into it. In this case, semantic information is incorporated into the syntactic representation on the form of attributed structural representation [8], [9], [18], [20]. The image features are represented by an alphabet of attributed entities, where the attributes represent some semantic parameters of the structural features. Moreover, the semantic information of the relationships among the image features is represented by the attributes associated with the relations between their corresponding entities. This approach for image representation has shown to provide compact, concise, and powerful representation that is capable of comprehending all the information contents of the images.

In this paper, we propose a general image understanding system. A block diagram of the system is shown in Fig. 2. The proposed system utilizes attributed relational graph (ARG) as a powerful tool for visual knowledge representation, and performs the analysis and understanding tasks on the extracted attributed relational graph representation of images.

Manuscript received April 8, 1985; revised January 29, 1986. Recommended for acceptance by Y. T. Chien. This work was supported by the Office of Naval Research under N00014-79-C-09574.

M. A. Eshera is with the Department of Artificial Intelligence, Martin Marietta Laboratories, Baltimore, MD 21227.

K. S. Fu was with the School of Electrical Engineering, Purdue University, West Lafayette, IN 47907. He is now deceased.

IEEE Log Number 8609320.

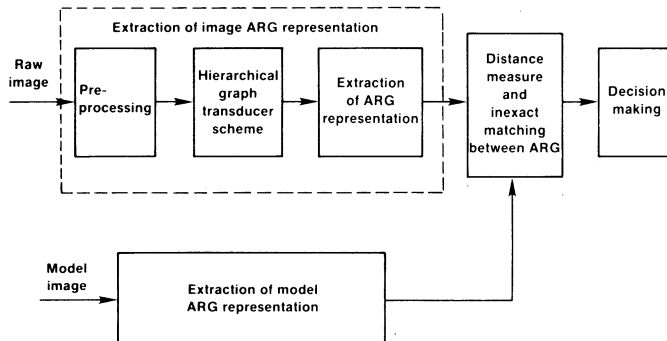


Fig. 2. Block diagram of the proposed image understanding system.

An attributed relational graph (ARG) is a relational structure which consists of a set of nodes and a set of branches representing the relations between the nodes. Both nodes and branches may have some attributes assigned to them. Usually, nodes are used to represent some objects or parts of objects in the image, while their properties are assigned as attributes to their respective nodes. The relations between two objects are represented by attributed branches between the corresponding nodes. A formal general definition of attributed relational graph (ARG) is given in [3].

At the representation extraction stage, the system utilizes a hierarchical multilayer scheme [6], for the extraction of a global representation in the form of ARG from images. The input to this scheme is an image as defined over a set of image primitives which is obtained by simple physical measurements on real images, it can be as simple as the gray scale values of the image pixels. The input images are the result of some very elementary preprocessing operations, e.g., filtering, edge detection, and thinning. The scheme extracts the informative global features from the image, as defined by the structural alphabet of a hierarchical graph transducer. This transducer is basically a rule-based transformation implemented in bitwise operations. It performs a recursive symbolic mapping of the image information contents from an input alphabet of local primitives, which is usually extracted from the spatial-domain representation on single pixel level, into an output alphabet of image global features. The extracted alphabet is then used to produce the image global representation in the form of an attributed relational graph.

At the analysis and interpretation stage, the system utilizes an inexact matching between ARG's, in terms of a graph distance measure [3] to carry on the image understanding process, and accomplish some tasks of interest, such as locating some objects in the image.

Informally, a similarity, or a distance measure between two images (or subimages) is defined as the maximum number of similar features that are common between the two images, or the minimum changes that need to be performed on one image in order to produce the other image. The important question in practical applications is not whether two images (subimages or objects) are identical, but rather how similar they are to each other. Thus, the

noise and distortion in real images can be accommodated by specifying tolerance in the distance measure between images [13], [15], [16], [19]. Moreover, an interesting issue is to define and calculate a distance measure between an image and a part of an image, i.e., how similar an object is to a sub-image, so the system can deal with overlapped objects as well as noisy and distorted images. The matching between images is performed through the matching of their respective ARG representation, and defined in terms of a distance measure between the two ARG's [3], [16], [19].

The proposed image understanding system will be demonstrated by two application experiments, as will be shown in this paper. Experiment I concerns with locating objects in a scene composed of complex overlapped objects, while Experiment II deals with target detection in highly noisy and distorted synthetic aperture radar (SAR) images.

In Section II, we discuss the preprocessing and preliminary segmentation techniques used in our system. The extraction of an ARG representation from spatial-domain images is discussed in Section III. In that section, we present the basic concepts of the graph transducer and the multilayer hierarchical scheme [6] with emphasis on their practical utilization in our system. In Section IV, we briefly review the dynamic programming approach for calculating a global distance measure and finding the best inexact matching between attributed relational graphs [3], [4] and discuss its practical utilization in image understanding systems. Section V presents our experimental results and demonstrates the capabilities and the usefulness of the proposed system. Some concluding remarks and directions for future research are discussed in Section VI.

II. PREPROCESSING AND PRELIMINARY SEGMENTATION

The spatial-domain representation of an image is the form of raw-image representation, in which most practical image understanding systems receive their input data. Entities of the spatial-domain representation are pixels whose values represent the gray-scale value of a very local area in the image. Figs. 3, 4, and 5 show some examples of typical images which are analyzed by the proposed system. Images are usually corrupted by noise and distortion. Moreover, the data entities in the spatial domain image representation possess a very strict local nature.

The construction of a meaningful global representation from the input imagery data is presented in Section III. Nevertheless, some preprocessing is needed to prepare the input raw images for the hierarchical scheme used in Section III. In Section II-A, we present the preprocessing techniques which are utilized in Experiment I. In Section II-B, we discuss the SAR image data and the preprocessing techniques which we propose to handle the noisy nature of SAR images which are used in Experiment II.

A. Preprocessing of Multiobject Scenes

In Experiment I, we use very simple processing in the form of a conventional edge operator, namely, the Sobel

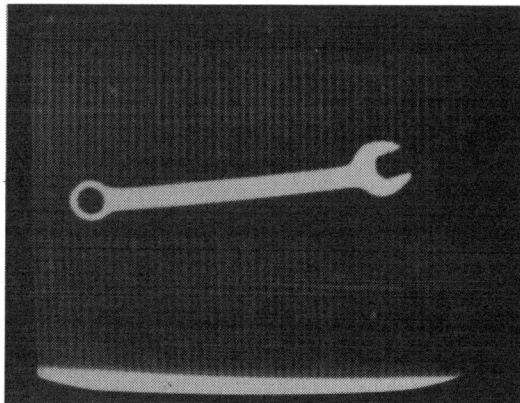


Fig. 3. An image of a model object.

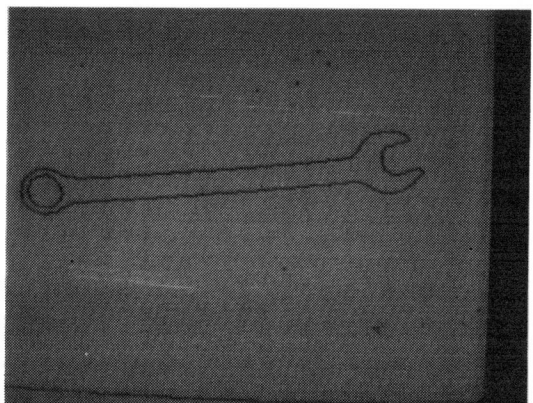


Fig. 6. Edge-based segmentation for the image of Fig. 3.

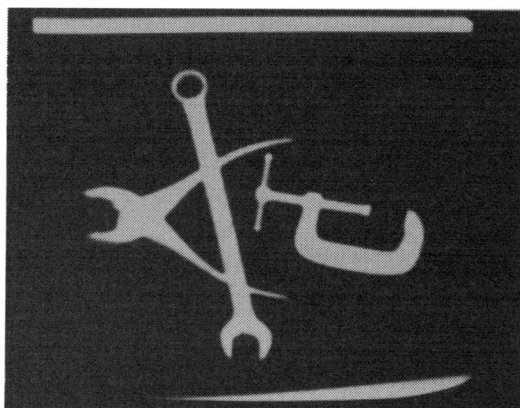


Fig. 4. An image of overlapping objects.

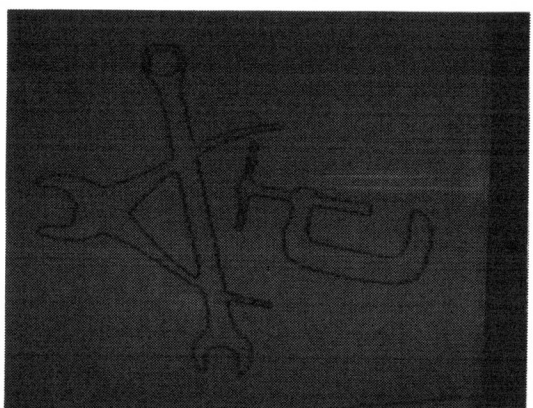


Fig. 7. Edge-based segmentation for the image in Fig. 4.



Fig. 5. The SAR gray scale image of Santa Barbara area.

edge-operator over 3×3 windows. The edge image is then segmented to extract the contours of the different regions in the images. The results of these operations on the images of Figs. 3 and 4 are shown in Figs. 6 and 7, respectively.

B. Preprocessing of SAR Images

The processing of aerial images, in general, and the synthetic aperture radar (SAR) images in particular, is a challenging task. This is not only due to their low signal-to-noise ratio, but also due to the vast diversion of the shape, the relative size, the nature, and the informative

features of the interesting objects in these images [2], [12]. Therefore, a relatively more sophisticated preprocessing technique is needed for the analysis of this type of images.

The multiresolution concept seems very appealing in the processing of aerial images, since one of the major characteristics of these images is the vast diversity of the objects that may exist in them. Some different objectives may have the same shape but different sizes or different relative dimensions. A clear example of such a case is the difference between highways and airport runways, where the size and the ratio of width-to-length become major discriminative features.

In order to efficiently perform the preliminary segmentation on the SAR images of Fig. 5, we utilize the multiresolution technique in a split-and-merge region-based segmentation and combine it with edge-based segmentation [11]. This is the main preprocessing technique which we utilize in this experiment, as we explain in more details in the remaining part of this section.

We assume that only the approximate size of objects in terms of the area represented by each pixel is known. Starting from the image with a suitable low resolution, we use a region-based segmentation, e.g., thresholding over the gray scale or the variance of the subimages, to obtain a low-resolution segmentation of the image. The results of this rough segmentation is then used for further

segmentation at finer levels of resolution. The formal algorithm for this technique is stated below as Algorithm II.1.

The idea behind this technique can be briefly explained in the following. We assume that the objects are composed of some wide regions of particular characteristic, such as texture, average gray level, variance, etc. The algorithm obtains a rough resolution of the input image based on the characteristic of the objects, as well as their approximate size; and it generates a rough segmentation of the image. This rough segmentation produces an image, say I_1 , which contains some candidate objects. Then, we obtain a finer resolution image, from the original image by doubling the resolution of the rough resolution image, and segment it as was done with I_1 , to produce an image, say I_2 . We mask I_2 by I_1 and pick up the pixels from I_2 which are adjacent to objects in I_1 and add them to the object regions, to produce the fine segmented image, say I_3 .

Algorithm II.1: Multiresolution Region-Based Segmentation

Purpose: To perform split-and-merge multiresolution region-based preliminary segmentation.

Input: A gray scale high resolution image.

Output: Segmented image containing the candidate objects.

Method:

- I. Obtain a suitable rough resolution image based on the approximate size of the interesting objects.
- II. Obtain a segmented image I_1 using some simple criterion, e.g., simple thresholding of the gray scale values.
- III. Obtain a finer resolution image, by doubling the resolution of I_1 .
- IV. Obtain a segmented image I_2 .
- V. Mask I_2 by I_1 in I_3 .
- VI. From I_2 , pick up the pixels which are adjacent to object pixels in I_3 and move them into I_3 .
- VII. Repeat step VI, until no more pixels can be added to I_3 .
- VIII. END ALGORITHM II.1

The objective of Experiment II is to detect some targets of interest in the SAR images. Specifically, in this experiment we aim at detecting airports in the SAR image of the Santa Barbara area. In general, airports are characterized, from their region-based features as relatively large and uniform flat regions which exhibit high reflectance. From their shape, i.e., edge-based features, they are characterized as consisting of some runways, usually two or more, that take the form of relatively long but not too narrow flat areas.

The results of applying the proposed technique and Algorithm II.1 to the Santa Barbara SAR image of Fig. 5 are shown in Figs. 8–11. The resulting image contains the candidate objects based on the region preliminary seg-

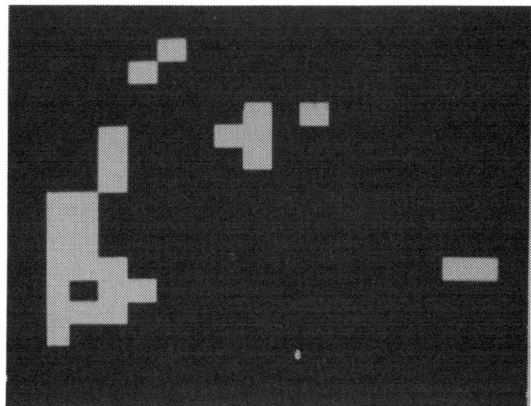


Fig. 8. Rough resolution image of the Santa Barbara SAR image.

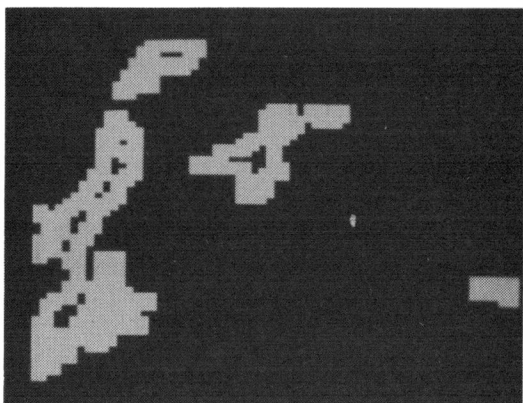


Fig. 9. Results of split-and-merge for the image of Fig. 8.

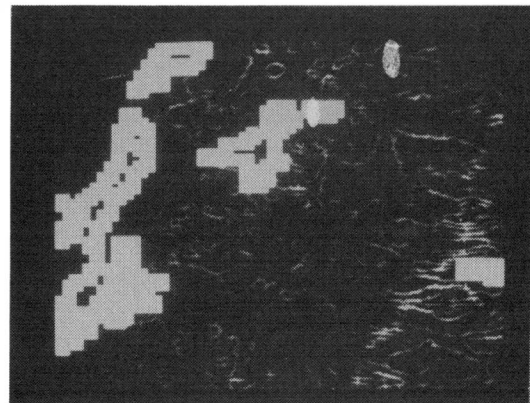


Fig. 10. Mask areas around candidate targets in the Santa Barbara SAR image.

mentation. Then the system focuses the attention on some mask areas around the candidate objects, and concentrates the edge-based segmentation within these areas. Fig. 12 shows the extracted edges within the focus of attention areas, using the Sobel local edge-operator. It can be easily seen from that figure that the extracted edges of the candidate targets are very noisy and distorted. Nevertheless, we utilize this preprocessing results to perform higher level analysis of the SAR images, where we extract an attributed relational graph representation from the image and perform the inexact matching of minimum global dis-



Fig. 11. Edge-based segmentation for the image in Fig. 10.

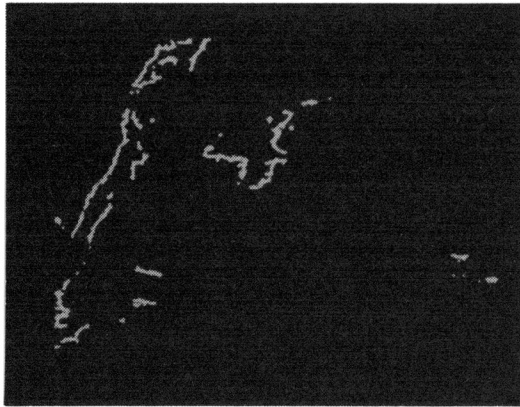


Fig. 12. Extracted edges within the focus of attention areas for the Santa Barbara SAR image.

tance between the extracted ARG representation of the image and the ARG representation of the target model as shown in the block diagram in Fig. 2 and explained in the following sections.

III. EXTRACTION OF IMAGE GLOBAL ATTRIBUTED REPRESENTATION

The proposed system utilizes a multilayer hierarchical scheme for the extraction of a global attributed symbolic representation from the input images. That scheme is proposed in details in [6] and reviewed briefly in Section III-A. The input to the scheme is in the form of an array of cells which take values over a very local input alphabet, as will be shown in Section III-B. A transformation mapping is driven by the input data in order to map its information contents from the input local alphabet into a global alphabet. This mapping takes place over a multilayer field of cells (or processors), whose elements are configured in a certain neighborhood configuration, as will be defined formally in Section III-A. The output alphabet of the hierarchical transformation at different layers in the scheme is designed according to the decomposition of the candidate complex objects into relatively simpler features (or image primitives). The output global alphabets which are used in the system are discussed in Section III-C. The neighborhood configuration among cells of the scheme

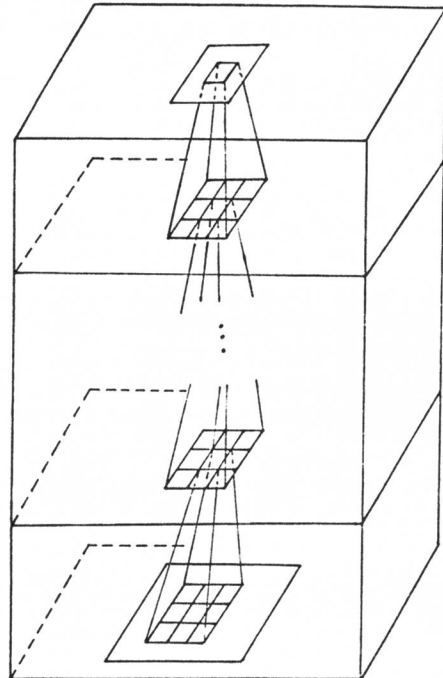


Fig. 13. Hierarchical scheme for the extraction of image global representation.

field, the adjacency predicate between output symbols, and the mapping functions of the hierarchical graph transducer are presented in Section III-D. The extraction of ARG representation from the field of the scheme is discussed in Section III-E.

A. Hierarchical Scheme for the Extraction of Attributed Relational Representation

The scheme proposed in [6] for the extraction of global attributed relational representation from spatial-domain images, is actually a parallel hierarchical scheme that consists of several layers, as shown in Fig. 13. Each layer has a field of cells that are connected according to a certain neighborhood configuration, as defined by a neighborhood predicate. In our work here, we will usually consider the eight-neighbor configuration, as shown in Fig. 14. However, in general the field can be connected in any arbitrary neighborhood configuration.

At each layer, the transducer performs a symbolic mapping of image information from a local alphabet into a relatively more global alphabet, i.e., the subimages over which the image alphabets are defined grow in size from one layer to the other. The bottom layer is considered the first, while the top layer is the last layer of the scheme. The input alphabet of the scheme, which is the input alphabet of its first layer, consists of a set of image primitives which are defined over very simple subimages, that could be as simple as single pixels. The scheme maps elements of the input alphabet into elements of an output alphabet, which are defined over global subimages. Formally, we define the multilayer graph transducer Γ of the form:

$$\Gamma = \{\Sigma_I, \Sigma_O, F, R, \Omega, \Phi\}$$

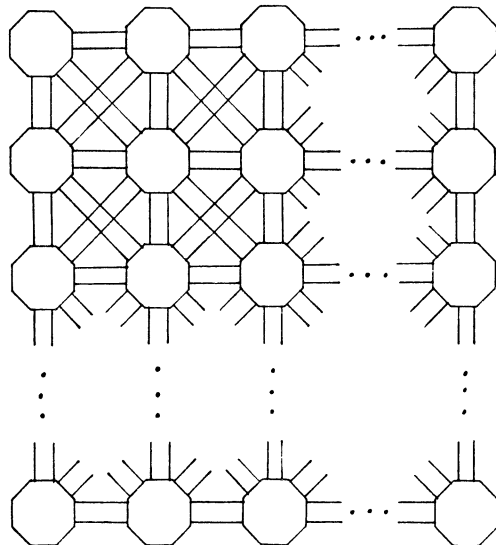


Fig. 14. A Graph transducer field in an eight-neighbor configuration.

where

- Σ_I is an input alphabet.
- Σ_O is an output alphabet, $\Sigma_O = \{\Sigma_O^1 \cup \Sigma_O^2 \cup \dots \cup \Sigma_O^L\}$, where L is the number of layers in the scheme.
- F is a multilayer field of cells, $F = F^1 \cup F^2 \cup F^3 \cup \dots \cup F^L$, where F^l , $1 \leq l \leq L$, is the l th layer in the field.
- R is a symmetric predicate that defines the adjacency between every two cells in F ; let S denotes the set of cell pairs as defined by R .
- Ω is a function that defines allowable pairs of alphabet symbols for every pair of adjacent cells in S .
- Φ ($\Phi(\sigma_i) \subseteq \Sigma_O$) is a function that defines the correspondence between subsets of Σ_O^i for every input symbol, and between alphabet symbols of different layers of the scheme.

The idea behind that scheme is based on the simplification of a complex object, or a global feature, by decomposing it into simpler subobjects, or some local features, with certain neighborhood relations between them. In other words, complex objects are decomposed, recursively, in a top-down fashion into sets of subobjects (or image features). The input alphabets, the output alphabets, and the mapping performed by the graph transducer are designed according to this recursive decomposition. For example, the boundary of any complex object can be decomposed down into a set of global features. These global features are composed of some local features, which are in turn composed of some relatively more local features and finally of some very basic image primitives.

B. The Input Alphabet

The input alphabet Σ_I , which is the input to the first layer of the scheme, consists of a set of local symbols in which the input images are presented. These symbols are

usually chosen to be easily measurable from the input image. An input image is presented to the multilayer scheme in the form of a field of cells that take values over that set of local symbols. The set of local symbols is taken as the input alphabet of the hierarchical graph transducer.

At the first layer of the scheme, the transducer performs a mapping of the image from input symbols into symbols of Σ_O^1 , which represents the alphabet of the transformation at the first layer. Each element of Σ_O^1 is composed of a group of elements from Σ_I which are arranged according to the neighborhood predicate R at this layer.

C. The Global Output Alphabet

In general, the hierarchical output alphabet is of the form: $\Sigma_O = \{\cup \Sigma_O^i | 1 \leq i \leq L\}$, where L is the number of layers in the scheme, and Σ_O^i is the alphabet at the i th layer of the scheme. Each element of the alphabet at the i th layer, Σ_O^i , is composed of a group of neighboring elements from the alphabet at the $(i - 1)$ th layer, Σ_O^{i-1} , in a recursive manner. The neighborhood configurations are defined by the neighborhood predicate R , as will be shown in Section III-D.

The output of the first layer is taken as input to the second layer of the scheme. In the second layer L_2 , the scheme maps elements of Σ_O^1 into elements of the subset Σ_O^2 , which represent the output alphabet of the transducer at this layer. Elements of Σ_O^2 are composed of elements from Σ_O^1 , according to the neighborhood predicate R . Thus, relatively more global features are extracted from the field of the first layer into cells of the field of the second layer.

In this section, we present the design of a hierarchical feature alphabet which is used by the multilayer scheme for the extraction of global image representation. We chose to represent complex objects by their contours. In this case, elements of the output alphabets of the hierarchical graph transformation are defined as line segments. Symbols of the alphabet at low levels in the scheme represent short lines, since the field cells at those levels cover relatively small areas in the image. On the other hand, symbols of the alphabet at higher levels represent relatively longer line segments, since cells of the scheme field at higher levels cover larger areas in the image.

The alphabet of the different layers of the transducer are defined to describe the features of a certain class of objects through the decomposition of these objects into subobjects and the recursive decomposition of global features into local features [6]. Each element in the alphabet of a certain layer represents a feature contained in the subimage covered by the cells of that layer.

The output alphabet of the first layer of the transformation, Σ_O^1 , is taken to represent the digitized line segments over 3×3 -pixel windows. While, elements of the alphabet of the second layer Σ_O^2 , are composed of those elements of Σ_O^1 which are laying in a group of neighboring cells as defined by the predicate R of the transducer. Elements of Σ_O^2 represent arbitrary line segments over 7×7 -pixel ($2^{2+1} - 1 \times 2^{2+1} - 1$) windows. Each 7×7 -

pixel window is formed from a central 3×3 -*pixel* window and its contour-surrounding 3×3 -*pixel* windows. That configuration provides overlapping among low level elements that form the same higher hierarchy element.

Similarly, elements of Σ_O^3 are composed of those elements of Σ_O^2 that are laying in a group of neighboring cells and forming longer lines, that are defined over larger windows, namely 15×15 -*pixel* ($2^{3+1} - 1 \times 2^{3+1} - 1$) windows. In general, elements of the alphabet of the i th layer Σ_O^i are composed of elements of the alphabet of the $(i-1)$ th layer, Σ_O^{i-1} , which lie in cells of the same neighborhood. A symbol $a_i \in \Sigma_O^i$ represents, in this case, a line segment that passes through the center cell of $(2^{i+1} - 1) \times 2^{i+1} - 1$ -*pixel* window.

The digitization noise is handled by the proposed approach through specification of the function Ω which defines pairs of alphabet symbols for every pair of adjacent cells in the neighborhood configuration. Moreover, the proposed hierarchical graph transducer can handle other noise and distortion by modifying the transformation mapping, as we will show later in this paper how the scheme can handle broken line segments in the images.

D. The Adjacency Predicate and Mapping Functions

The predicate R is a symmetric predicate which defines the neighborhood configuration of cells in the transducer field F . In other words, it specifies whether two cells in the field are adjacent or direct neighbors of each other. In general, the neighborhood relations among cells of the transducer field can be defined in any arbitrary configuration required, or the best suitable for characterizing a certain class of images. However, in most practical cases, we restrict the neighborhood relations between field cells into simple, e.g., four-neighbor or eight-neighbor, configuration.

In our experimental work, at the first layer we use the eight-nearest neighbors of each center cell to form nine cells neighborhood configurations. Each of those eight cells is said to be "adjacent" to the center cell and vice versa. The mapping function Ω at this layer defines pairs of possible adjacent output symbols for every pair of adjacent cells, while the function Φ defines the correspondence between input and output symbols. The detailed description of these mapping functions is given in [5]. At this layer, the graph transformation maps the image from the input alphabet into elements of Σ_O^1 . Each cell in this layer of the scheme represents a possible line segment which passes through this cell and lies in its surrounding 3×3 -*pixel* window. Thus, the transformation of the first layer maps the scope of the field cells from single pixel into 3×3 -*pixel* window.

In the second layer, the adjacency predicate R defines the 16 cells surrounding every 3×3 window of cells as the neighbors of the center cell of that window, forming a neighborhood configuration which has scope of 7×7 -*pixel* window, as shown in Fig. 15. Each of those cells is said to be "adjacent" to the center cell and vice versa. The mapping function Ω at this layer defines pairs of pos-

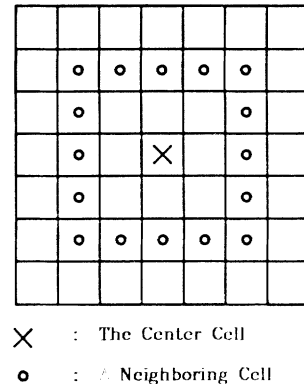


Fig. 15. A neighborhood configuration of the second layer in the hierarchical scheme. X : The center cell. O : A neighboring cell.

sible adjacent symbols, from Σ_O^2 , for every pair of adjacent cells. The function Φ defines the correspondence between symbols of Σ_O^1 and Σ_O^2 for the center cells of every neighborhood configuration. The transformation at this layer maps the image features from Σ_O^1 , whose elements are defined over 3×3 windows of image pixels, into Σ_O^2 , whose elements are defined over 7×7 -*pixel* windows.

In general at the i th layer, the transformation performs mapping of the scope of the field cells from $(2^i - 1) \times (2^i - 1)$ windows of image pixels into $(2^{i+1} - 1) \times (2^{i+1} - 1)$ windows of image pixels. The adjacency predicate R within the i th layer defines the 4×2^i cell surrounding every $(2^i - 1) \times (2^i - 1)$ window as the neighbors of the center cell of that window, where each of these cells is called "adjacent" to the center cell of the window. The transformation at this layer maps the image features from elements of Σ_O^{i-1} , which are defined over $(2^i - 1) \times (2^i - 1)$ window of pixels into more global symbols of Σ_O^i , which are defined on larger windows of $(2^{i+1} - 1) \times (2^{i+1} - 1)$ image pixels. The mapping algorithm, Algorithm III.1, is presented briefly at end of this section, while some more details and examples are given in [6].

This hierarchical mapping continues in the scheme with growing size alphabet until it satisfies the size of the global features, which are sought to be extracted from the image, or theoretically until the size of the alphabet covers the whole image. The objective of this scheme is not to attempt to recognize whole complex objects, but rather to extract the global symbolic representation which can then be represented by an attributed relational graph (ARG) for further higher level analysis, as we will demonstrate in the experimental results in this paper.

Algorithm (III.1) Symbolic Mapping

Purpose: To map image information contents from a set of image primitives defined over local subimages into a set of global entities defined over larger subimages.

Input:

- 1) A graph transducer T
- 2) A low level image representation defined by entities from the input alphabet Σ_I over an input image field of cells P .

Output: A global description of the input image, defined by the output alphabet Σ_o over the transducer field F .

Method:

- I. Construction of the graph representation in the transducer field
 - (i) FOR all $f \in F$ DO {
 - FOR all $\sigma_o \in \Sigma_o$ DO {
 - Insert a labeled node σ_o in cell f
 - (ii) FOR all $(f_i, f_j) \in S$ DO {
 - FOR (σ_i in cell f_i , .AND. σ_j in cell f_j) DO {
 - IF $(\sigma_i, \sigma_j) \in \Omega(f_i, f_j)$ THEN
 - Connect nodes σ_i and σ_j by a branch
 - $\beta(\sigma_i, \sigma_j) \in B$
- II. Input image into the transducer field
 - (i) FOR all $p_i \in P$ DO {
 - Designate a cell $f_i \in F$
 - (ii) FOR all $f_i \in F$ DO {
 - Eliminate all nodes of the subset $\{\Sigma_o - \Phi(\sigma_i)\}$ from f_i , where $\sigma_i \in \Sigma_i$ is the input symbol in p_i
- III. FOR all $f \in F$ DO {
 - FOR all $(f_i, f_j) \in S$ DO {
 - FOR σ_i in cell f_i DO {
 - IF (f_i contains more than one node, and there does not exist at least one node σ_j such that $\beta(\sigma_i, \sigma_j) \in B$) THEN
 - Eliminate node σ_i
- IV. Repeat Step III until no more nodes can be eliminated from their field F
- V. END ALGORITHM (III.1).

E. The Extraction of ARG Representation

The multilayer hierarchical scheme, discussed above, performs the mapping of the image information contents from the spatial domain into the alphabet Σ_o of global image symbolic representation. For the experiments presented in this paper, elements of the alphabet Σ_o represent digitized line segments of different length and orientation. Elements of Σ_o at layer i , $\Sigma_o^i \subseteq \Sigma_o$, denotes line segments of different length, while elements of the same layer denote line segments of different orientation. The output field of the scheme is an array of cells which take values over Σ_o . Nevertheless, the same information contained in that array can be better represented by an attributed relational graph (ARG) of the form presented in [3].

The extraction of an ARG from the field of the hierar-

chical scheme is a straightforward conversion of the image representation from the field of the hierarchical scheme into a graph form, as shown in Section V. An ARG consists of a set of attributed nodes and a set of attributed branches. The nodes represent different features in the image with attributes representing the properties of the corresponding features. The attributed branches represent the relations between the different features in the image. In Sections V-A and V-B, we present the ARG representations which are extracted from both Experiment I and Experiment II. In the next section, we discuss the analysis of images through a distance measure and inexact matching between the ARG extracted from these images.

IV. INEXACT MATCHING OF ATTRIBUTED RELATIONAL GRAPHS

In [3] and [4], Eshera and Fu proposed an efficient approach for calculating a distance measure between two ARG's, in the general form, and finding the best inexact matching configuration between components of the two ARG's. The best inexact matching between two ARG's is the matching configuration between components of both ARG's such that the overall distance measure between the two ARG's possesses a global minimum. The overall distance measure between two ARG's is defined in terms of the incremental distance (or local weights) between their respective components, i.e., between the nodes and the branches of the two ARG's. The local weights between nodes or branches are assigned as functions of the respective features or relations which are represented by those nodes or branches, respectively. It is needless to say that these weights of the local error-transformations of node or branch insertion, deletion, or substitution are basically design parameters that are problem dependent, as we will illustrate in Section V with our experimental results.

The global distance measure between two ARG's is formally defined as the cost of minimum total-cost sequence of weighted error-transformation which when performed on one of the ARG (or a subgraph of it), will produce the other ARG. Therefore, the calculation of such a distance measure between two ARG's involves not only finding any sequence of error-transformation, but also finding the sequence which possesses minimum total cost. The approach generates a state-space representation of the problem, in which each state denotes the inexact matching of a pair of subgraphs from the two ARG's. The initial state in this representation scheme denotes the starting of the matching process, and the final states are those states denoting the successful completion of matching both ARG's. The transition from a state to another state represents the embedding of a pair of matched components into the already matched subgraphs; the weight on this branch denotes the incremental cost due to this intermediate matching operation. A heuristic criterion is defined to govern the possible next matched pairs of components which can be performed at each state in the representation scheme. The concepts and the details of this criterion are presented

in [3]. The state-space representation scheme is, in general, in the form of a directed branch-weighted lattice.

The minimization aspect of the distance measure between ARG's is converted into a shortest-path problem over the directed acyclic branch-weighted lattice from the initial state to a state in the set of final states. This optimization problem, for that type of lattice, can be solved by dynamic programming in time linearly proportional to the number of states in the lattice.

The above technique is utilized for finding the matching configuration of minimum global distance between two attributed relational graphs for locating objects in an overlapped multi-object scene, in Experiment I, and for target detection in SAR images, in Experiment II. The attributed nodes in the ARG's represent different image features in the images with their attributes representing some properties of these features, such as the length of line segments or the span of curve segments. The branches between nodes in the ARG represent the attributed relations between the respective features represented by those nodes, as will be shown in Sections V-A and V-B for Experiment I and Experiment II, respectively.

V. EXPERIMENTAL RESULTS

The proposed image understanding system is implemented on VAX-11/780 and tested by two experiments. Experiment I is concerned with locating objects in a scene composed of complex overlapped objects, while Experiment II deals with target detection in highly noisy and distorted synthetic aperture radar (SAR) images. In this section, we present the results of both experiments.

A. Locating Objects in Multiobject Scenes

In Experiment I, we choose node and branch alphabets as shown in Fig. 16. The nodes are chosen to represent straight Line segment (L) with length (l) as an attribute, Arc segment (A) with length (l) and span (d) as attributes, and closed Curves (C) with contour length (l) as an attribute. A branch between two nodes in the ARG represents the relationship between the two features represented by these two nodes. Branches are taken to correspond to Joint relation (J) with attribute as the joint angle (θ), Intersection relation (I) with the angle of intersection (θ) as an attribute, and the relation between non-joint and nonintersecting, i.e., apart or Facing (F), features with attribute (d) represents the distance between the two center points of the two entities.

The set of image global features extracted from the single object model image of Fig. 3 is shown in Fig. 17(a), while the set of relations between those features are shown in Fig. 17(b). The ARG representation of that image is shown in Fig. 18. Similarly, the set of image global features extracted from the multiobject image of Fig. 4, and the set of relations between those features of that image are shown in Fig. 19. The ARG representation of the multiobject image is shown in Fig. 20.

For this experiment, we choose the weights of insertion and deletion of different nodes and branches of the attrib-

Node Attribute Alphabet

Entity	Attributes
Straight Line Segment L	Length l
Arc Segment A	Length l Span d
Closed Curve C	Contour l

$$A = \{L(l), A(l, d), C(l)\}$$

Branch Attribute Alphabet

Relation	Attributes
Joint J	Angle ν
Intersect I	Angle ν
Facing F	Distance d

$$E = \{J(\nu), I(\nu), F(d)\}$$

Fig. 16. Node and branch attribute alphabets.

GLOBAL FEATURES EXTRACTED FROM THE TRANSFORMATION FIELD :

feature no.	type	attributes
1	l	144
2	a	54, 18
3	l	136
4	a	33, 24
5	a	39, 18
6	a	36, 27
7	c	15

RELATIONS BETWEEN THE EXTRACTED FEATURES :

relation	type	attributes
1, 2	J	130
2, 3	J	165
3, 4	J	140
4, 5	J	50
5, 6	J	40
6, 1	J	150
1, 3	F	12
2, 7	F	3
7, 5	F	153
4, 6	F	33

Fig. 17. Image features and relations extracted from the single-object image of Fig. 3.

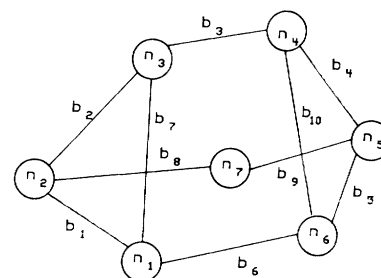


Fig. 18. Attributed relational graph representation for the single-object image of Fig. 3.

GLOBAL FEATURES EXTRACTED FROM THE TRANSFORMATION FIELD

feature no.	type	attributes
1	l	132
2	a	36, 24
3	a	39, 18
4	a	33, 24
5	l	136
6	a	51, 15
7	c	12
8	a	90, 84
9	a	87, 81
10	a	93, 84
11	a	39, 36
12	a	45, 21
13	a	42, 39
14	a	93, 84
15	a	39, 36
16	l	60
17	l	27
18	l	57
19	l	18
20	a	21, 18
21	a	21, 18
22	l	21
23	a	24, 21
24	a	30, 27
25	l	18
26	l	45
27	l	24

RELATIONS BETWEEN THE EXTRACTED FEATURES :

relation	type	attributes
1, 2	j	150
2, 3	j	40
3, 1	j	40
4, 5	j	145
5, 10	i	60
10, 11	j	140
11, 13	f	33
13, 12	j	30
12, 11	j	30
9, 10	j	10
1, 14	i	80
1, 20	f	18
20, 21	j	110
21, 1	f	24
21, 22	f	3
22, 23	j	90
23, 14	j	100
24, 18	f	6
18, 17	j	90
18, 23	f	6
17, 16	j	90
16, 15	j	75
15, 27	f	12
27, 26	j	90
26, 16	f	15
26, 25	j	90
25, 18	j	90
1, 9	i	70
8, 14	j	10
1, 10	i	70
1, 6	j	170
1, 5	f	12
5, 6	j	150
2, 4	f	27
3, 7	f	144
7, 6	f	3
8, 5	i	70
5, 14	i	70
5, 9	i	70
9, 8	j	100
19, 20	f	3
19, 17	f	21

Fig. 19. Image features and relations for the multiobject image of Fig. 4.

uted relational graphs, as shown in Tables I and II, for the insertion and deletion, respectively, while Tables III and IV show the weights of substitution (or relabeling) of nodes and branches, respectively. The physical meaning of these weights of error-transformations can be clearly

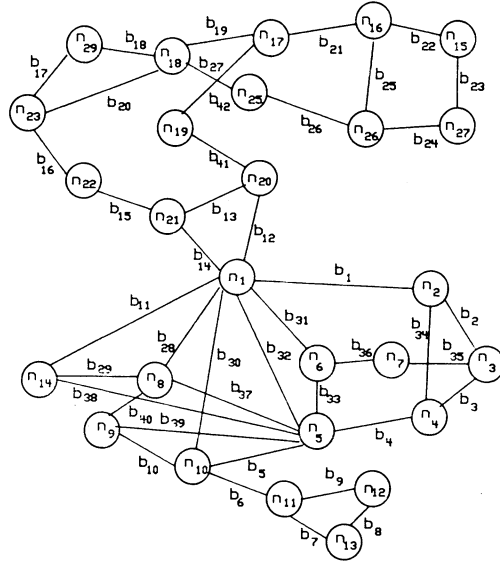


Fig. 20. Attributed relational graph representation for the multiobject image of Fig. 4.

TABLE I
ASSIGNED WEIGHTS OF NODE INSERTION AND DELETION FOR EXPERIMENT I

Node	Insertion	Deletion
(L : l_1)	l_1	l_1
(A : l_1, d_1)	l_1	l_1
(C : l_1)	l_1	l_1

TABLE II
ASSIGNED WEIGHTS OF BRANCH INSERTION AND DELETION FOR EXPERIMENT I

Branch	Insertion	Deletion
(J : v_1)	v_1	v_1
(I : v_1)	v_1	v_1
(F : d_1)	d_1	d_1

TABLE III
ASSIGNED WEIGHTS OF NODE SUBSTITUTION FOR EXPERIMENT I

	(L : l_1)	(A : l_1, d_1)	(C : l_1)
(L : l_2)	$ l_1 - l_2 $	$ l_1 - l_2 + d_1$	$l_1 + l_2$
(A : l_2, d_2)	$ l_1 - l_2 + d_2$	$ l_1 - l_2 + d_1 - d_2 $	$ l_1 - l_2 + d_2$
(C : l_2)	$l_1 + l_2$	$ l_1 - l_2 + d_1$	$ l_1 - l_2 $

seen from the physical meaning of the attributes of the different entities of the attributed relational graphs. The approach proposed in [3] is used to locate the object of

TABLE IV
ASSIGNED WEIGHTS OF BRANCH SUBSTITUTION FOR EXPERIMENT I

	(J : v ₁)	(I : v ₁)	(F : d ₁)
(J : v ₂)	v ₁ -v ₂	v ₁ -v ₂	v ₂ + d ₁
(I : v ₂)	v ₁ -v ₂	v ₁ -v ₂	v ₂ + d ₁
(F : d ₂)	v ₁ + d ₂	v ₁ + d ₂	d ₁ -d ₂

THE BEST INEXACT MATCHING BETWEEN THE TWO ARG'S U AND V

NODE-PAIRS

GRAPH V	GRAPH U
n1	n5
n2	n6
n3	n1
n4	n2
n5	n3
n6	n4
n7	n7

BRANCH-PAIRS

GRAPH V	GRAPH U
b1	b33
b2	b31
b3	b1
b4	b2
b5	b3
b6	b4
b7	b32
b8	b36
b9	b35
b10	b34

THE MINIMUM DISTANCE = 84

Fig. 21. Matching configuration and minimum distance for the two ARG's of Figs. 18 and 20.

Fig. 3 in the multiobject overlapped scene of Fig. 4, by calculating the graph distance measure between their respective ARG's, which are shown in Figs. 18 and 20, and finding the best inexact matching configuration which possesses minimum global distance between the two attributed relational graphs. The results of this experiment are shown by the matching configuration shown in Fig. 21.

B. Target Detection in SAR Images

In this experiment, Experiment II, we choose node alphabet to represent arbitrary straight line segments (L), with the length (l) as their attributes. Branches of the ARG representation in this experiment represent the relationships between the line segments which are represented by the nodes. The branches are taken to correspond to the following possible relations: Parallel (P) with attribute as the distances (d_1, d_2) between the two line segments, Joint (J) with attribute as the joint angle (θ), and (O) with at-

GLOBAL FEATURES EXTRACTED FROM THE TRANSFORMATION FIELD :

feature no.	type	attributes
1	1	40
2	1	12
3	1	10
4	1	12
5	1	30
6	1	20
7	1	30
8	1	60
9	1	40
10	1	16
11	1	16
12	1	36
13	1	8
14	1	16
15	1	10
16	1	10
17	1	16
18	1	14
19	1	20
20	1	16
21	1	18
22	1	32
23	1	10
24	1	8
25	1	20
26	1	16
27	1	12
28	1	16
29	1	20
30	1	10

RELATIONS BETWEEN THE EXTRACTED FEATURES :

relation	type	attributes
1, 2	J	70
2, 3	P	8, 12
3, 4	P	16, 10
1, 5	P	24, 10
1, 6	J	30
1, 7	O	70, 75
7, 8	J	75
7, 10	P	10, 10
8, 9	J	80
8, 11	P	16, 8
9, 12	P	12, 4
12, 13	P	0, 60
13, 14	J	75
14, 15	J	90
15, 16	J	45
16, 17	P	20, 0
16, 18	P	22, 4
17, 18	J	135
12, 19	O	54, 90
13, 19	O	60, 110
19, 20	P	26, 0
11, 21	P	72, 0
21, 22	J	90
22, 23	J	90
23, 24	J	90
22, 24	P	16, 8
25, 26	J	75
26, 27	J	75
27, 28	O	10, 45
28, 29	J	90
29, 30	J	90
21, 29	P	20, 0
21, 30	O	12, 90

Fig. 22. Image features and relations for the SAR image of Santa Barbara area.

tributes (d, θ), where d is the distance and θ is the angle between the two line segments.

The set of image global features extracted from the SAR image of the Santa Barbara area is shown in Fig. 22(a), while the set of relations between these features are shown in Fig. 22(b). The ARG representation of that image is shown in Fig. 23. The sets of attributed features and re-

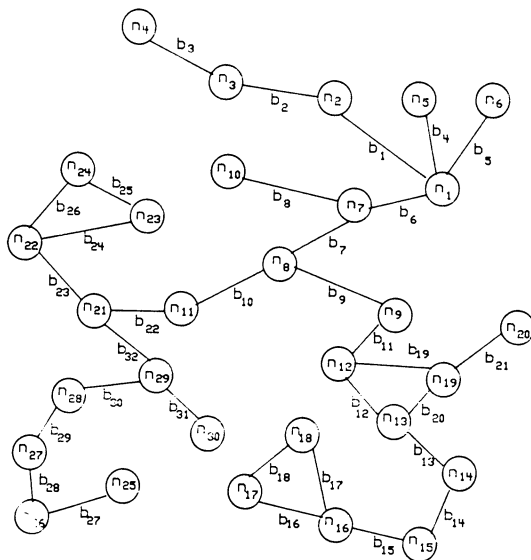


Fig. 23. Attributed relational graph representation for SAR image of Santa Barbara area.

TABLE V
ATTRIBUTED FEATURES FOR A MODEL OF AN AIRPORT

Pattern No.	Type	Attributes
n ₁	l	10
n ₂	l	30
n ₃	l	30
n ₄	l	10
n ₅	l	30
n ₆	l	10
n ₇	l	10
n ₈	l	10
n ₉	l	20
n ₁₀	l	10
n ₁₁	l	20
n ₁₂	l	30

lations of a model of an airport are shown in Tables V and VI, while its ARG representation is shown in Fig. 24.

The weights of insertion and deletion of different nodes and branches of the attributed relational graphs, in this experiments are shown in Table VII and Table VIII, for insertion and deletion, respectively. Tables IX and X show the weights of substitutions (or relabeling) of nodes and branches, respectively. The technique proposed in [3] is, then, used to find the best inexact matching configuration between ARG representation of the SAR image and that of a model target airport, and calculating the global distance measure between the two ARG's. The results of this experiment are shown in Figs. 25 and 26.

TABLE VI
ATTRIBUTED RELATIONS BETWEEN IMAGE FEATURES FOR A MODEL OF AN AIRPORT

Relation	Type	Attributes
1, 2	j	90
2, 3	j	120
3, 4	j	90
4, 5	j	90
5, 6	j	60
6, 7	j	90
7, 8	j	90
8, 9	j	90
9, 10	j	90
10, 11	j	90
11, 12	j	90
1, 7	p	50, 0
1, 12	j	90
2, 12	p	10, 0
3, 5	p	10, 0
4, 12	p	40, 30
6, 8	p	10, 0
9, 11	p	10, 0

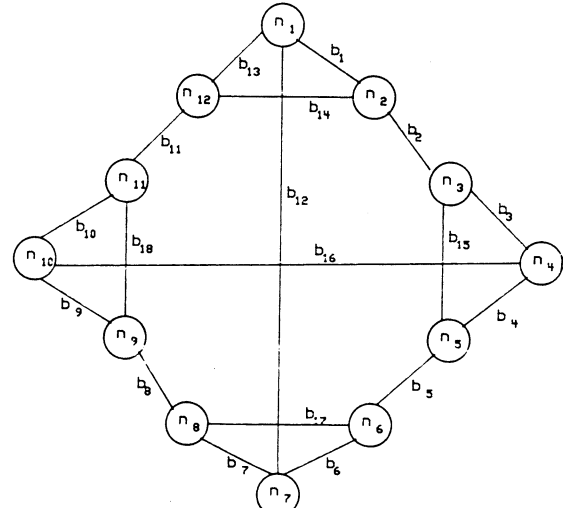


Fig. 24. Attributed relational graph representation for a model of an airport.

VI. CONCLUDING REMARKS

For an image understanding system to be useful in performing practical tasks, it must be able to handle its input as real-world images in their raw form, which are usually

TABLE VII
ASSIGNED WEIGHTS OF NODE INSERTION AND DELETION FOR EXPERIMENT II

Node	Insertion	Deletion
(L : ℓ_1)	ℓ_1	ℓ_1

TABLE VIII
ASSIGNED WEIGHTS OF BRANCH INSERTION AND DELETION FOR EXPERIMENT II

Branch	Insertion	Deletion
(J : v_1)	v_1	v_1
(O : d_1, v_1)	$d_1 + v_1$	$d_1 + v_1$
(P : d_1, d_2)	$d_1 + d_2$	$d_1 + d_2$

TABLE IX
ASSIGNED WEIGHTS OF NODE SUBSTITUTION FOR EXPERIMENT II

(L : ℓ_1)	
(L : ℓ_2)	$ \ell_1 - \ell_2 $

TABLE X
ASSIGNED WEIGHTS OF BRANCH SUBSTITUTION FOR EXPERIMENT II

	(J : v_1)	(O : d_1, v_1)	(P : d_{11}, d_{12})
(J : v_2)	$ v_1 - v_2 $	$ v_1 - v_2 + d_1$	$v_2 + d_{11} + d_{12}$
(O : d_2, v_2)	$ v_1 - v_2 + d_2$	$ v_1 - v_2 + d_1 - d_2 $	$ 90 - v_2 + d_{11} - d_{12} $
(P : d_{21}, d_{22})	$v_1 + d_{21} + d_{22}$	$ 90 - v_1 + d_{21} - d_1 $	$ d_{11} - d_{21} + d_{22} - d_{12} $

in the spatial-domain representation. On the other hand, an image understanding system must comprehend the image information contents in a global form, since the output of the system is the result of some decision making operation, which is usually based on the global information contents of the image. In this paper, we have proposed a comprehensive image understanding system, which can handle input images in the spatial-domain form; performs some simple preprocessing; extracts the image global representation in the form of an ARG; pursues the image understanding task on the extracted ARG representation; and finally, draws its conclusive decision based on the results of a global distance measure and inexact matching of ARG's. The proposed system possesses several powerful features, which we discuss below.

THE BEST INEXACT MATCHING BETWEEN THE TWO ARGs U AND V

NODE-PAIRS

GRAPH	V	GRAPH	U
n1		n23	
n2		n24	
n3		*	
n4		*	
n5		n25	
n6		*	
n7		*	
n8		n28	
n9		n29	
n10		n30	
n11		n21	
n12		n22	

BRANCH-PAIRS

GRAPH	V	GRAPH	U
b1		b25	
b2		*	
b3		*	
b4		*	
b5		*	
b6		*	
b7		*	
b8		b30	
b9		b31	
b10		b33	
b11		b23	
b12		*	
b13		b24	
b14		b26	
b15		*	
b16		*	
b17		b29	
b18		b32	

THE MINIMUM DISTANCE = 219

Fig. 25. Matching configuration and minimum distance for the two ARG's of Fig. 23 and 24.

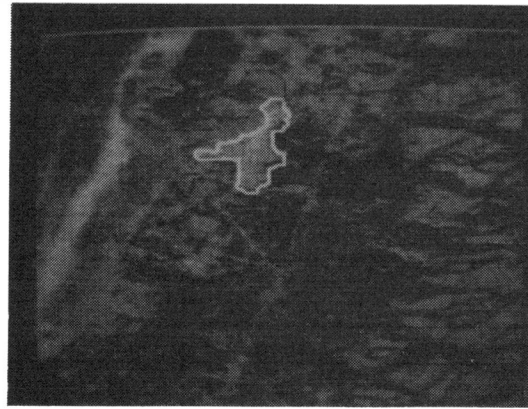


Fig. 26. Approximate location of an airport in the SAR image of Fig. 5.

- The system accepts its input as spatial-domain images, which is the form of raw images usually available from image digitizing peripherals.
- To capture the global information contents of the image, the system utilizes a powerful knowledge representation scheme in the form of attributed relation graphs, which is shown to be the most appropriate representation scheme to cope with the richness of imagery data and to preserve all its information contents, such as symmetry, closure, connectivity of objects, etc. It also combines the parametric (i.e., the decision theoretic) and the structural

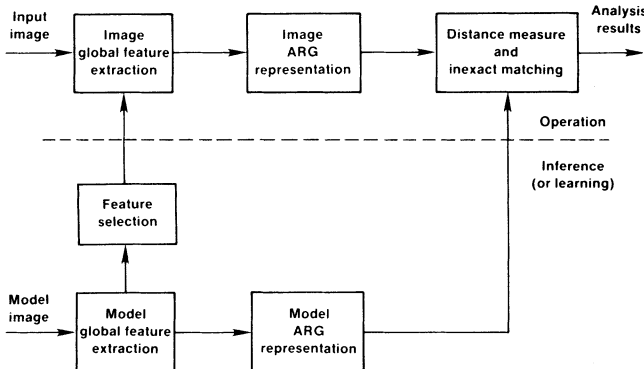


Fig. 27. Block diagram of a more general image understanding system.

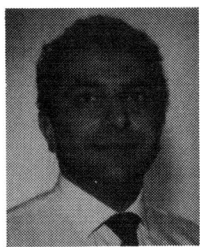
representation approaches in an attributed relational representation.

- The proposed system provides a hierarchical multilayer scheme to bridge the traditional gap between "low-level" image processing and "high-level" image understanding. This scheme is a rule-based approach which uses both model-driven and data-driven concepts to perform a symbolic mapping of the image data from the spatial-domain representation into a global representation.
- The system performs the high-level analysis on the extracted global representation, i.e., the ARG, through an efficient approach for calculating a global distance measure and finding the best inexact matching configuration between those representations.
- The proposed system handles noise, distortion, and ambiguity, which usually exist in real images by modeling them into the symbolic mapping in the multilayer scheme, as shown in the broken lines in our experiments, and also through the distance measure and the error handling capability of the inexact matching technique.
- The multilayer scheme and the inexact matching technique are both suitable for parallel processing hardware implementation, which is an important practical concern of the system, especially for its use in real time applications [1].
- The hierarchical graph transducer used in our system utilizes the model-object information to restrict the alphabet of image features into only those features which are obtained from the recursive decomposition of complex model objects into image primitives. The inference of such an alphabet of features can be done manually or automatically by a training procedure. The transducer is capable of performing the required inference in a straightforward fashion by first considering the set of all image features over the different subimages. In this case, the mapping is mainly driven by the input data only. The extracted image features are then considered as the required alphabet to be used later in the technique. However, the set of all features must be large and therefore, the technique will be slow in performing the learning task. A faster, or more intelligent, learning technique needs to be developed to infer the alphabet of the global representation.
- The inference procedure suggested above can be in-

corporated with the rest of our system in a more general system, as shown in Fig. 27. The system possesses the learning capability through the inference procedure to build up the alphabet of image features and primitives. Both the image feature alphabet and the attributed relational graph representation of the model-objects are extracted from the model images during the learning phase. In the operation phase, the system utilizes the alphabet of image features inferred from the model images to extract the attributed relational graph representation of any given image.

REFERENCES

- [1] N. Ahuja and S. Swamy, "Multiprocessor pyramid architectures for bottom-up image analysis," *IEEE Trans. Pattern Anal. Machine Intell.*, vol. PAMI-6, pp. 463-475, July 1984.
- [2] M. A. Eshera, H. S. Don, K. Matsumoto, and K. S. Fu, "A syntactic approach for SAR image analysis," in *Proc. ONR Workshop Statistical Image Processing and Graphics*, Luray, VA, May 24-27, 1983.
- [3] M. A. Eshera and K. S. Fu, "A graph distance measure for image analysis," *IEEE Trans. Syst., Man, Cybern.*, vol. SMC-14, pp. 398-408, May/June 1984.
- [4] —, "A measure of similarity between attributed relational graphs for image analysis," in *Proc. Seventh Int. Conf. Pattern Recognition*, Montreal, P.Q., Montreal, Canada, July 30-Aug. 2, 1984, pp. 75-77.
- [5] M. A. Eshera, "Image understanding by attributed symbolic representation and inexact matching of attributed graphs," School Elec. Eng., Purdue Univ., West Lafayette, IN, Tech. Rep. TR-EE 85-8, Apr. 1985.
- [6] M. A. Eshera and K. S. Fu, "A hierarchical scheme for extracting attributed symbolic representation for image understanding," 1986, submitted for publication.
- [7] K. S. Fu, *Syntactic Pattern Recognition and Applications*. Englewood Cliffs, NJ: Prentice-Hall, 1982.
- [8] —, "Attributed grammars for pattern recognition—A general (syntactic-semantic) approach," *Proc. IEEE*, pp. 18-27, 1982.
- [9] —, "A step towards unification of syntactic and statistical pattern recognition," *IEEE Trans. Pattern Anal. and Machine Intell.*, vol. PAMI-5, pp. 200-205, Mar. 1983.
- [10] K. Fukunaga, *Introduction to Statistical Pattern Recognition*. New York: Academic, 1972.
- [11] S. L. Horowitz and T. Pavlidis, "Picture segmentation by a directed split-and-merge procedure," in *Proc. Second Int. Conf. Pattern Recognition*, Aug. 1974, pp. 424-433.
- [12] J. S. Lee, "A simple speckle smoothing algorithm for SAR images," *IEEE Trans. Syst., Man, Cybern.*, vol. SMC-13, pp. 85-89, Jan./Feb. 1983.
- [13] S. Y. Lu and K. S. Fu, "A sentence-to-sentence clustering procedure for pattern analysis," *IEEE Trans. on Syst., Man, Cybern.*, vol. SMC-8, May 1978.
- [14] T. Pavlidis, *Structural Pattern Recognition*. New York: Springer-Verlag, 1977.
- [15] A. Sanfelix and K. S. Fu, "Distance between attributed relational graphs for pattern recognition," *IEEE Trans. Syst., Man, Cybern.*, vol. SMC-13, May/June 1983.
- [16] L. G. Shapiro and R. M. Haralick, "Structural descriptions and inexact matching," *IEEE Trans. Pattern Anal. Machine Intel.*, vol. PAMI-3, pp. 504-519, Sept. 1981.
- [17] W. H. Tsai and K. S. Fu, "Error-correcting isomorphism of attributed relational graphs for pattern analysis," *IEEE Trans. Syst., Man, Cybern.*, vol. SMC-9, pp. 757-768, Dec. 1979.
- [18] —, "Attributed grammar—A tool for combining syntactic and statistical approaches to pattern recognition," *IEEE Trans. Syst., Man, Cybern.*, vol. SMC-10, pp. 873-885, Dec. 1980.
- [19] —, "Subgraph error-correcting isomorphism for syntactic pattern recognition," *IEEE Trans. Syst., Man, Cybern.*, vol. SMC-13, pp. 48-67, Jan./Feb. 1983.
- [20] K. C. You and K. S. Fu, "A syntactic approach to shape recognition using attributed grammars," *IEEE Trans. Syst., Man, Cybern.*, vol. SMC-9, pp. 334-345, June 1979.



M. A. Eshera (S'82-M'85) received the B.S.E.E. degree in electronics and communication engineering from Cairo University, Giza, Egypt, the M.Sc. degree in electrical and computer engineering from Drexel University, Philadelphia, PA, in 1980, and the Ph.D. degree from Purdue University, West Lafayette, IN, in 1985.

He is currently a scientist in the Department of Artificial Intelligence at Martin Marietta Laboratories, Baltimore, MD, working in the area of image analysis and understanding, computer vision, and artificial intelligence. In 1985, he was a Member of Technical Staff with Bell Communications Research, Piscataway, NJ, working on system automation for network characterization and planning. From 1981 to 1984, he was a researcher in the Advanced Automation Research Laboratory at Purdue University. From 1978 to 1980, he was a Research and Teaching

Assistant at Drexel University. He served as a consultant for both industrial and governmental organizations, and has held scholarships and assistantships throughout his education. His research interests include computer vision, image analysis and understanding, image processing, robotics vision, graph algorithms, combinatorial optimization, network planning, knowledge representation, and machine intelligence. He has published several papers on these topics.

Dr. Eshera is a member of Sigma Xi, Tau Beta Pi, SPIE, and the IEEE Computer Society.

King-Sun Fu (S'56-M'59-SM'69-F'71), for a photograph and biography, see this issue, p. 603.
